Colloid Polym Sci 277:627–636 (1999)

ORIGINAL CONTRIBUTION

G. Stakkestad
B. Grung
J. Sjöblom
T. Sigvartsen

Surface chemistry of lanthanum chromite powders II. Multivariate data modelling of the isoelectric point by the use of surface composition data achieved from X-ray photoelectron spectroscopy measurements

Received: 8 October 1998
Accepted in revised form: 27 January 1999

G. Stakkestad · T. Sigvartsen
Prototech AS, Fantoftveien 38
N-5036 Fantoft, Norway

B. Grung · J. Sjöblom (✉)
Department of Chemistry
University of Bergen
N-5007 Bergen, Norway

Abstract Electrophoretic mobility measurements and X-ray photoelectron spectroscopy (XPS) analysis have been performed on several lanthanum chromite powders with different dopants. Principal component analysis of both deconvoluted XPS data and differentiated overall XPS spectra showed a clustering of the powders. From loading plots it was seen that high amounts of La and O on the surface gave highest isoelectric points (IEP). Partial-least-squares, multivariate response modelling was used to calibrate the IEPs from both deconvoluted XPS data and from differentiated overall XPS spectra. The best model was obtained when second-order differentiated overall XPS spectra were used, with an average predictive error of pH ± 0.25. This is promising considering that the IEP has been determined with an accuracy of pH_{IEP} ± 0.3. When deconvoluted data was used, the average predictive error rose to pH ± 1.1. It is therefore an advantage to use multivariate data analysis which is a nonsubjective latent variable decomposing technique in contrast to deconvolution which is an even more time-consuming method for calibration of IEP values from XPS.

Key words Lanthanum chromite powder – Electrophoretic mobility – X-ray photoelectron spectroscopy – Multivariate data analysis

Introduction

Production of gas-tight, defect-free interconnects for solid oxide fuel cells (SOFC) is important regarding electrical output and lifetime. We have reported [1–2] on the electrical conductivity, microstructure and mechanical properties of Ca- and Sr-doped $LaCrO_3$, interconnects for SOFCs. Relative density, secondary phases and grain boundary layers were found to have an impact on the electrical conductivity and the mechanical strength of these materials.

Defect-free ceramic composites with fine-grain microstructure can be obtained by processing colloidal particles [3]. During the mixing, dispersing, forming and firing steps good colloidal control and hence knowledge of the surface chemistry of the components is important. This enables one to understand and control the adsorption of dispersants, binders, pressing aids and sintering agents on the powders. Sintering of the green body to maximum density depends on the surface free energy available in the powder, and the particle packing efficiency. In a previous report [4] we used particle size distribution data together with calcination temperature in the multivariate modelling of the surface area of different lanthanum chromite powders.

In these measurements we have focused on the surface chemistry of the same powders. Electrophoretic mobility was used to determine the isoelectric point (IEP) of the different powders and to investigate the existence of positive and negative surface groups. These measurements were also used to obtain information on the double-layer properties of each powder. X-ray photoelectron spectroscopy (XPS) was used to characterise the chemical composition on the powder surface.

Deconvolution is the method most used in XPS for the interpretation and qualification of spectra containing multiple peaks [5–7]. Deconvolution has been shown to be useful in XPS because it is a straightforward technique and much information on peak positions for the elements in different chemical states has been published [8]. Its main disadvantage is that the results are not necessarily unique [9–10]. If uncertainty exists in the number of peaks in a spectrum, or in the widths of various peaks, there may be many different combinations of component peaks, which reconstruct the data within experimental error.

Multivariate analysis has been shown to be a very powerful method of data analysis, applicable to XPS [11–14]. Multivariate analysis is an efficient tool for interpreting the vast amount of information yielded by modern spectroscopic techniques. By using latent variable methods such as principal component analysis (PCA) and partial least squares (PLS) the multivariable spectroscopic data can be reduced to a number of variables that are more suitable for human examination. Furthermore, the latent variable methods decompose the original collinear data to a set of orthogonal variables that can be used in regression analysis. Thus, it is possible to use complete instrumental profiles (such as XPS spectra) in regression calculations. In spite of the data reduction obtained using these methods, information is not lost in the way it is when only small fractions of spectra are interpreted by deconvolution.

The intention of this study is to model the IEPs as a function of the surface composition from the XPS analysis. The IEP can be an important parameter for optimisation of ceramic process control. By being able to model IEPs from spectroscopic data a more time-consuming electrophoretic mobility measurement step can be cancelled. The environmental issue is also important here since dissolution of lanthanum chromite powder in water before analysing can then be omitted. The motivation for doing this is also that it can help in interpreting the type of atomic composition on the complex lanthanum chromite powder surface that is decisive with regard to the variation of the IEP.

Materials and methods

Chemicals and powders

The lanthanum chromite powders were supplied by two manufacturers.

Powder A (Pyrox, France): 20% Ca-doped lanthanum chromite ($La_{0.8}Ca_{0.2}CrO_3$), produced by the conventional solid-state reaction method (mixing of oxides and firing at about 1200 °C).

Powder B (Praxair Speciality Ceramics, USA): produced by the combustion spray pyrolysis method. For the B powders we specified the amount and type of dopants.

The characteristics of the lanthanum chromite powders are shown in Table 1.

Electrophoretic mobility

Electrophoretic mobility was determined by the microelectrophoresis technique using a Zetasiser 4, Malvern Instruments, UK. A mobility spectrum is obtained from the Doppler shift resulting from the light scattering of the particles.

Pro analysis grade NaCl, NH_3 and CH_3COOH were used throughout the experiments. The water was purified by a Seralpur Pro 90 water purification system (Seral), before ultrasonic treatment for removal of oxygen.

The dry powder was suspended by ultrasonication for 5 min in electrolyte solution with adjusted pH. The powder concentration was about 0.05 wt%. All measurements were made at 24 ± 0.1 °C, and at constant ionic strength (10^{-2} M NaCl).

Most ceramic powders are used as received in the ceramic process and we believe that processing problems are related to the surface chemistry of the as-received powders. Ceramic processing of lanthanum chromite powders is usually done in organic media where dissolution from the powder surface is insignificant compared to in water. The electrophoretic mobilities reported here are in aqueous media, measurements are performed 5 min after solution in water, and will therefore not correspond to equilibrium conditions. The uncertainty in the pH_{IEP} values measured here is taken into account in the Results and Discussion.

X-ray photoelectron spectroscopy

An XPS spectrometer (Vacuum Generators Micro Lab III) was used to analyse the chemical composition of the surface film of the different powders. The spectrometer was equipped with a Mg and Al K α X-ray source and a hemispherical analyser. The powder was mounted on an aluminium support covered by a thermoplastic. Three replicates of overall spectra and detail spectra were analysed. We used the VGS 5000 data system to curve-fit the data. Briefly the curve fitting provided by this system subtracts a Shirley-type of background and is accomplished using a nonlinear least square method. The quality of the fit is determined by the value of chi

Table 1 Characteristics of the lanthanum chromite powders: powder A (Pyrox, France) and powder B (SSC, USA)

Powder	Nominal	Synthesis	Sintering aid	Calc. Temp. (°C)
A1	$La_{0.8}Ca_{0.2}CrO_{2.9}$	Solid-state reaction	Y_2O_3	1200
B1	$La_{0.8}Ca_{0.2}CrO_{2.9}$	Spray pyrolysis		650
B2	$La_{0.85}Ca_{0.15}CrO_{2.93}$	Spray pyrolysis		650
B3	$La_{0.8}Ca_{0.2}CrO_{2.9}$	Spray pyrolysis		1150
B4	$LaCr_{0.9}Ni_{0.1}O_{2.95}$	Spray pyrolysis		650
B5	$LaCr_{0.9}Zn_{0.1}O_{2.95}$	Spray pyrolysis		650
B6	$La_{0.9}Sr_{0.1}Cr_{0.9}Ni_{0.1}O_{2.9}$	Spray pyrolysis		1000
B7	$La_{0.9}Sr_{0.1}Cr_{0.9}Cu_{0.1}O_{2.9}$	Spray pyrolysis		1000
B8	$La_{0.9}Sr_{0.1}Cr_{0.9}Mg_{0.1}O_{2.9}$	Spray pyrolysis		1000

squared. A 90° angle to the detector was chosen to optimise the intensity to the detector, and to do simple reproducible analysis. The XPS peaks are of a Gaussian–Lorentzian mix. Theoretical sensitivity factors are used which may not give the optimum composition.

The PCA model

PCA is an exploratory data analysis method [15–16]. By projecting the measured data onto latent variables that are linear combinations of the measured ones, informative low-dimensional plots can be obtained. These plots display information about the variable and sample correlation. In PCA, the latent variables are called principal components (PCs). The PCs are chosen so as to explain as much of the variation in the data as possible while being orthogonal to each other. For most data, substantial data complexity reduction can be obtained by PCA. Since the number of underlying real factors having a significant influence upon the system is usually low, it is often possible to construct a small number of such "super variables" that contain all the information in the data.

The PLS model

In response modelling, where the covariance between two sets of variables **X** (data matrix) and **Y** (response matrix) is analysed, the principal component is often not the ideal latent variable. The aim is to extract the information in **X** that covaries as much as possible with the information in **Y**. This is done by decomposing the **X** space so that the latent variables describe the **Y** space as well as possible. PLS is a much used method for this purpose [17–18]. PLS decomposes the collinear **X** to a set of uncorrelated latent variables on which the regression coefficient, **b**, is calculated. Unlike many other regression techniques, variable selection is therefore unnecessary.

Preprocessing of the data

Prior to the construction of the PCA and the PLS model preprocessing of the curve-fitted data was done in order to have comparable contributions of the different variables to the models. Both the X-block and Y-block matrices were mean-centred and standardised before PCA and PLS algorithms were used.

Different types of preprocessing of the XPS spectra were tested and the effect on the PCA classification of the replicates, and the predictive power from PLS were followed. Normalisation of the spectra was performed to make the size of samples comparable. The variables are divided by their sum so that the variables sum to 1 for each sample. Differentiation is a preprocessing technique used to remove background and to enhance selectivity in spectral profiles. Second-order differentiation removes a linear baseline shift and changes a curved second-order polynomial background into a baseline shift [19].

The data analysis was performed using Sirius for Windows version 1.5 Pattern Recognition System, Norway.

Results

Electrophoretic mobility

In Fig. 1 the electrophoretic mobility versus pH for powders A1 and B1 is shown. The IEPs for the two 20% Ca-doped powders coincide at a value of 5.6. When Ca doping is reduced to 15% (powder B2) the IEP is raised to 6.8 (Fig. 2). For 10% Ni- or Zn-doped powders (B4 and B5) pH_{IEP} increases to 7.6 (Fig. 3). Figure 4 shows that almost all the Sr-doped powders have IEPs at 3.7 except Sr/Ni double-doped powder (B6), which has an IEP value of 4.1. The electrophoretic mobility for all powders is at a maximum at about pH 3 and decreases towards pH 2. The decrease in electrophoretic mobility below pH 3 can

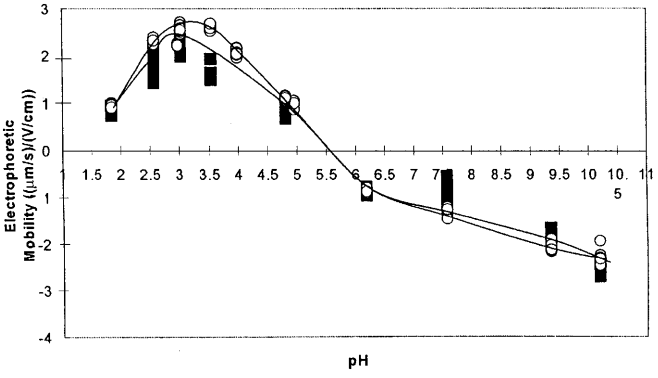

Fig. 1 Electrophoretic mobility as a function of pH for differently synthesized $LaCrO_3$ powders A1(■) and B1 (○)

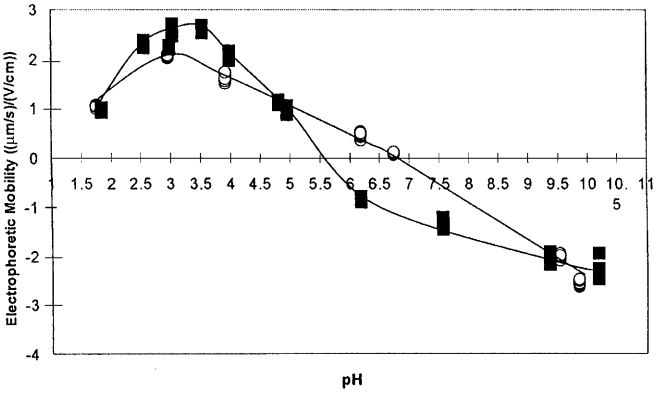

Fig. 2 Electrophoretic mobility as a function of pH for different amounts of dopants on $LaCrO_3$ powders B1 (■) and B2 (○)

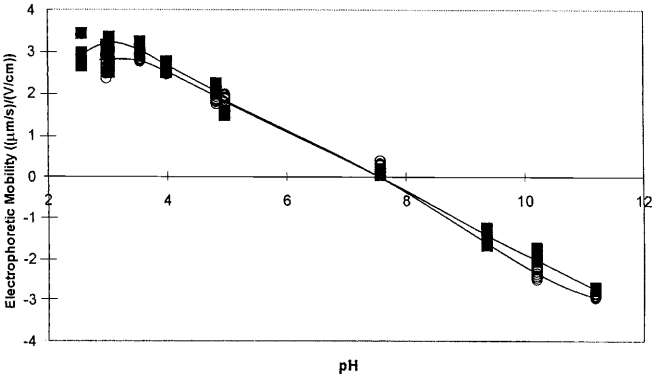

Fig. 3 Electrophoretic mobility as a function of pH for differently doped $LaCrO_3$ powders B4 (■) and B5 (○)

be interpreted as an increase in chromium dissolution from the surface in a strong acidic environment [20], resulting in a more negative surface.

Deconvolution of XPS

A typical XPS spectrum of lanthanum chromite powder is shown in Fig. 5. The atomic ratios determined from deconvolution of the XPS spectra of the different powders are summarised in Table 2, together with the pH_{IEP} results.

PCA of deconvoluted data from XPS

To establish a relationship between the IEP of the lanthanum chromite powders and their surface composition from visual inspection of Table 2 can be tedious. A faster and easier way to develop informative plots on the relation between IEPs of the powders and their surface composition is to perform an explorative PCA with the lanthanum chromite powders as objects and the

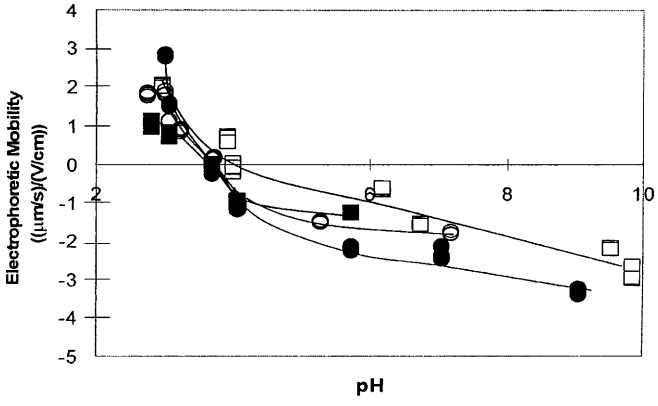

Fig. 4 Electrophoretic mobility as a function of pH for differently doped and double-doped $LaCrO_3$ powders B3 (■), B6 (□), B7 (●) and B8 (○)

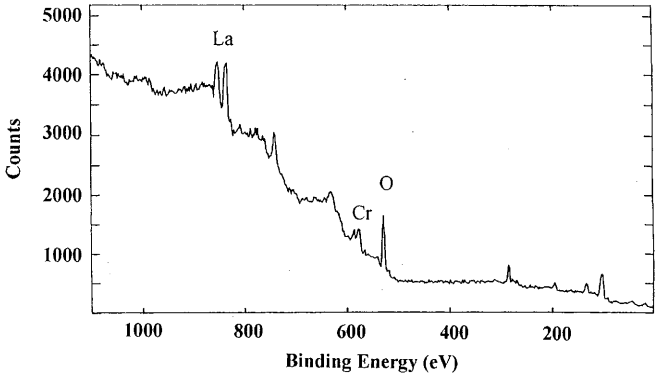

Fig. 5 Example of an X-ray photoelectron spectroscopy (*XPS*) spectrum of doped $LaCrO_3$

Table 2 pH_{IEP} and atomic ratios from deconvoluted X-ray photoelectron spectroscopy (*XPS*) spectra of the different powders[a]

Powder	pH_{IEP}	Atomic ratios from deconvoluted XPS			
		La/Cr	O/Cr	Ca/Cr	Sr/Cr
A1	5.6	2.33	9.09	0.32	–
B1	5.6	1.92	6.67	0.32	–
B2	6.8	2.17	6.25	0.25	–
B3	3.7	1.03	5.26	–	0.47
B4	7.6	2.86	8.33	–	–
B5	7.6	4.16	10.0	–	–
B6	4.1	1.21	5.26	–	0.35
B7	3.7	1.67	7.14	–	0.51
B8	3.7	1.47	5.26	–	0.37

[a] Estimated errors for pH_{IEP} ±0.3

variables form Table 2. The data were standardised and mean-centred prior to the PCA. Two PCs explained 63.3% of the total variance in the data where PC1 explained 53.1%, and PC2 explained 10.2%. The score plot is shown in Fig. 6. The angle and distance between two objects (powders) in the score plot relative to the origin is a measure of their similarity. The powders seem to distribute into three classes. Class 1 contains B8, B7, B6 and B3, class 2 contains B1, B2 and A1 and class 3 contains B4 and B5. There is a tendency that the powders with the lowest IEPs are distributed on the negative side of PC1, namely class 1, while the powders with the highest IEPs are on the positive side of PC1. Powders with intermediate measured IEP values have approximately zero score on PC1.

The loading plot, Fig. 7, gives an indication of the correlation pattern between the variables. Variables with a small angle in the plot are highly positively correlated. A 90° angle indicates no correlation, and an angle of 180° reveals that the variables are negatively correlated. From this IEP can be said to clearly positively correlate to the atomic ratio La/Cr, meaning that when La content increases in the powder surface the IEP increases. O/Cr also strongly positively correlate to IEP, while dopant atomic ratios, Sr/Cr and Ca/Cr negatively correlate to IEP.

A combination of the score plot and loading plot, a so-called biplot, Fig. 8, gives information of which variables characterise the different powders. B4 and B5 are the powders with the highest IEPs (7.6), and they highly positively correlate to relative amounts of La and O on the surface and subsequently high IEPs, while B3, B6, B7 and B8 negatively correlate to La/Cr and O/Cr.

Mutlivariate regression of IEP from deconvoluted XPS results

By using multivariate response modelling (PLS) we wanted to check if it was possible to model the IEP of

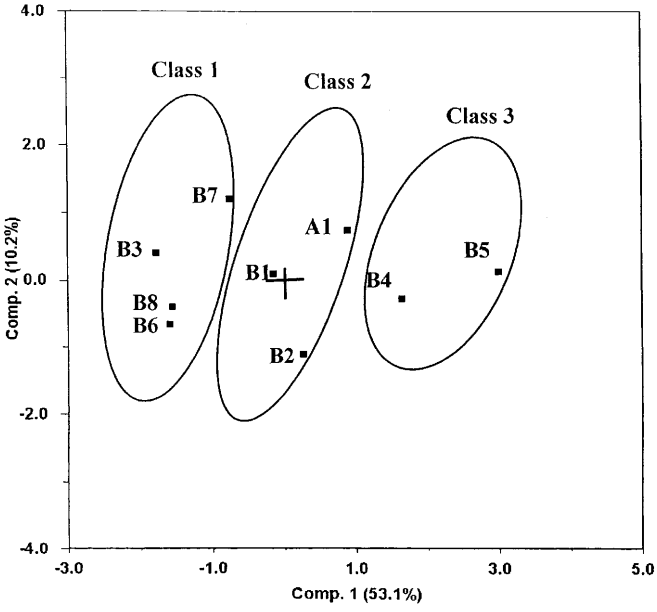

Fig. 6 Principal component analysis (*PCA*) score plot of deconvoluted XPS data and pH_{IEP}. PC1 explains 53.1% and PC2 explains 10.2% of the total variance. *Full line circles* (—) indicate class 1, 2 and 3 of the powders

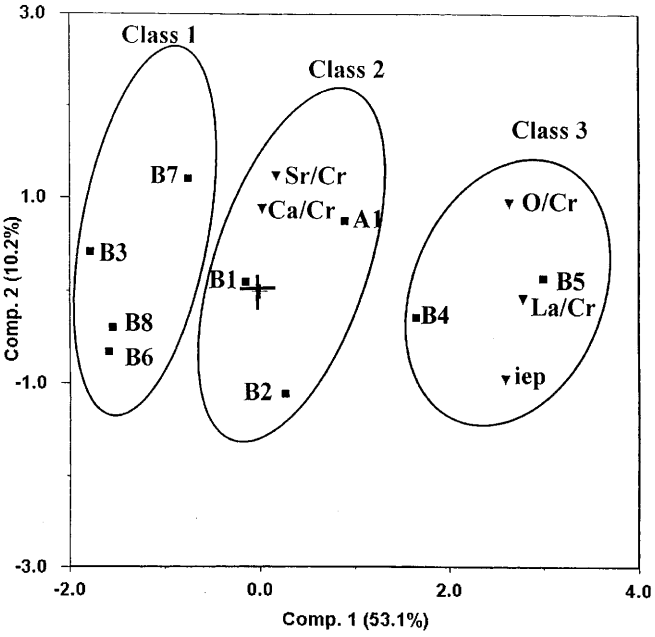

Fig. 8 PCA bi-plot of deconvoluted XPS data and pH_{IEP}, PC1 explains 53.1% and PC2 explains 10.2% of the total variance. *Full line circles* (—) indicate class 1, 2 and 3 of the powders

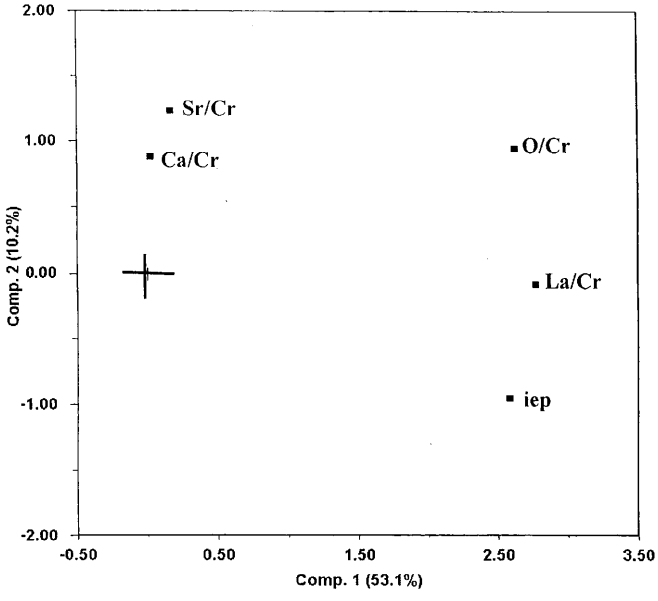

Fig. 7 PCA loading plot of deconvoluted XPS data and pH_{IEP}. PC1 explains 53.1% and PC2 explains 10.2%

the powders by the use of the deconvoluted XPS data. Only B powders were used in the modelling, since A1 is synthesised differently from the other powders. Eight PLS models were constructed leaving out one of the powders each time as an independent validation sample. The one-component model constructed then predicted the independent validation sample. Table 3 summarises results from the different one-component models. The average predictive error of the validation sample is pH ± 1.1.

Table 3 Measured and predicted isoelectric point (*IEP*) of the eight partial-least-squares (*PLS*) models from deconvoluted XPS data

Sample[a]	Measured IEP	Predicted IEP
B1	5.6	5.1
B2	6.8	5.0
B3	3.7	4.0
B4	7.6	6.3
B5	7.6	10.2
B6	4.1	4.1
B7	3.7	5.4
B8	3.7	4.4

[a] Independent validation sample

IEPs are not well predicted by using XPS deconvoluted data. An explanation for this may be that important information remains in the parts of spectra which are not used. Using multivariate PLS regression allows us to analyse and model the response with overall XPS spectra as inputs. No subjective criterion is used in latent variable decomposing in contrast to deconvolution analysis. Instead, the covariance structure between spectra and the response is used.

PCA of XPS spectra

PCA was performed on the overall spectra of the nine powders (×3 replicates = 27 spectra), to see if the powder replicates distribute well.

Normalising the spectra shows that a reduction from 1100 to 2 variables preserves 79.3% of the total variance in the data (Fig. 9). PC1 explains 52.7% while PC2 explains 26.6% of the variance. The powders are well distributed in the score plot. There seems to be a clustering of the powders into four classes. Class 1 contains A1 and B3, class 2 contains B1, B2 and B8, class 3 contains B4 and B5, and class 4 contains B6 and B7.

Second-order differentiation with 11 points in the filter was tried as a preprocessing technique prior to extraction of PCs from the XPS spectra. (The 11-point filter was chosen as the best for these types of spectra after PCA and PLS analysis of 5, 11 and 15 points had been tested on the spectra.) Figure 10 reveals the score plot, with as much as 83.7% of the total variance explained with the use of two latent variables. The powders are clustered into three classes. Class 1 contains B3, B6, B7, B8 and A1, class 2 contains B1 and B2, and class 3 contains B4 and B5. One replicate of B1 shows anomalies from the other, as it seems to fit into class 1 instead of class 2. This B1 spectrum is therefore characterised as an outlying sample. Differentiating the spectra prior to PCA shows almost similar clustering/classification as the XPS curve-fitted data.

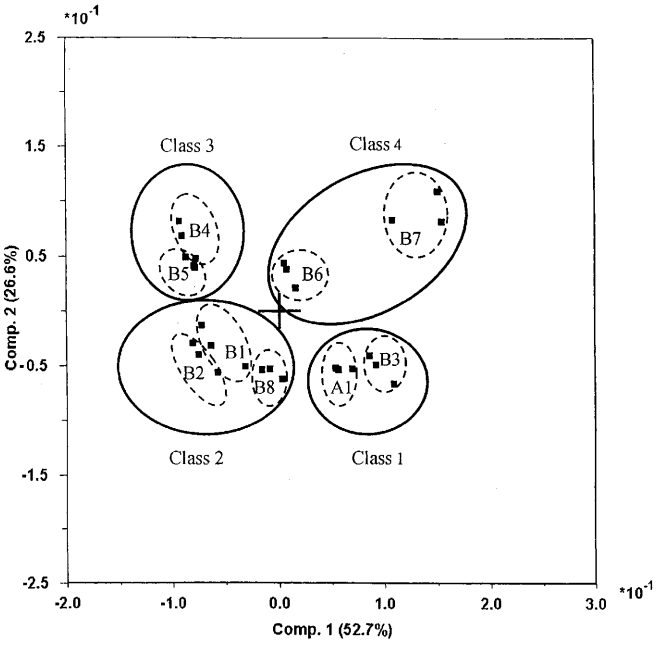

Fig. 9 PCA score plot of normalised XPS overall-spectra, PC1 explains 52.7% and PC2 explains 26.6%. *Full line circles* (—) indicating class 1, 2, 3 and 4, while *dotted circles* (- - - -) enclose the three replicates of each powder

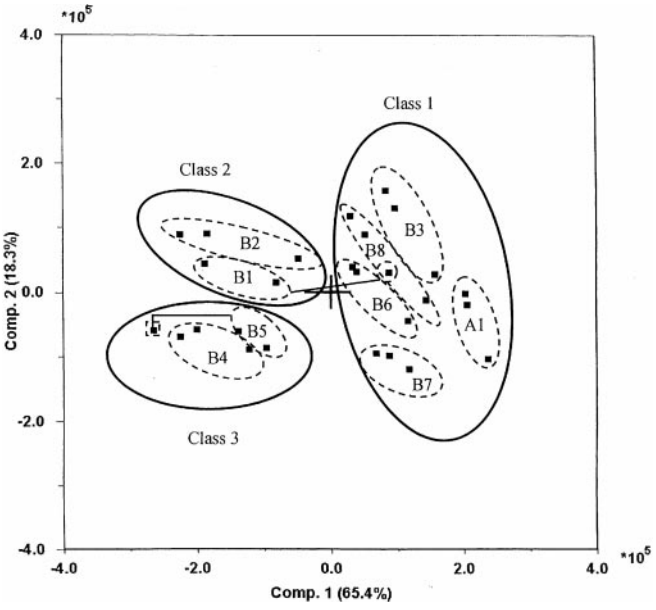

Fig. 10 PCA score plot. Differentiated XPS overall spectra, PC1 explains 65.4% and PC2 explains 18.3%. *Full line circles* (—) indicate class 1, 2 and 3, while *dotted circles* (- - - -) enclose the three replicates of each powder

We see that the three replicates seem to have a time-dependent factor, which may be due to the fact that all three replicates were put into vacuum at the same time and analysed one by one. It is clear from the PCA plot in Fig. 10 that this dwell times in vacuum has interfered with the powder sample surface composition. Others [14] have also found that the sample surfaces change while they are in the vacuum environment of the instrument. The change is not uniform among the samples but there is a tendency that O content decreases.

Multivariate regression of IEP from XPS spectra

PLS modelling of the IEP was also tested with the overall XPS spectra, with second-order differentiation as a preprocessing technique. A1 was kept out of the models since this powder is synthesised differently than the others. Eight models were extracted where one powder at the time was left out to be used as an independent validation sample for the model. Only the first replicates were used in the models since time-dependent variations were observed in the replicates. Table 4 shows the results for the eight one-component models produced from the first replicate of powders B1-B8.

An average predictive error of pH $\pm$ 0.6 is achieved. This is a good result considering that the estimated error in the IEP is $pH_{IESP} \pm 0.3$. Further work on optimisation of XPS spectra uptake methods is necessary to be able to improve the models predictive power even more.

Knowing that the three replicates of the powders are not optimally achieved, a model containing all 24 B samples was produced. All B samples were then predicted by this one-component PLS model. For each powder the replicate with the lowest prediction error was chosen as the input for eight new models using the previously described way of leaving out one sample. This was done to demonstrate the power of the PLS modelling provided that the input spectra are of good quality.

Now the average predictive error is even more improved to pH ± 0.25. This shows that multivariate data analysis is a powerful tool in combination with XPS.

Figure 11 reveals a plot of the regression coefficients for the B5 model in Table 5. A comparison of the regression coefficients to the XPS spectra (Fig. 5) shows which parts of the spectra are important for the model. The size of the coefficients shows that a (834 and 851 eV) and O (531 eV) peaks give the highest contribution from the XPS spectra in the modelling of the IEP. Cr, C and Si (impurities) also contributed to the model.

A closer look at the oxygen peak in the regression plot (Fig. 12a) shows that the highest negative regression coefficients are at binding energies of 533 and 534 eV. The IEPs are calculated by multiplying the regression coefficients with the differentiated spectral data. Figure 12b reveals the second-order differentiated oxygen peak for three powders with different IEP values. We see that the increasing negative contribution at binding energies of 533 and 534 eV (hence a positive contribution to the model) correlates to an increase in the IEP. Figure 12c shows these XPS oxygen peaks before preprocessing. Note that the peaks of the raw spectra become negative after the double-differentiating procedure.

Table 4 Measured and predicted IEP for the eight PLS one-component models produced from the first replicate of the XPS overall spectra

Sample[a]	Measured IEP	Predicted IEP
B1	5.6	7.0
B2	6.8	6.0
B3	3.7	3.6
B4	7.6	7.1
B5	7.6	6.7
B6	4.1	4.1
B7	3.7	4.5
B8	3.7	3.7

[a] Independent validation sample

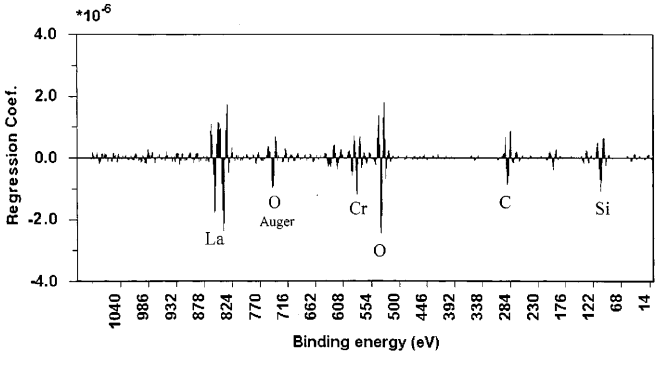

Fig. 11 Regression coefficient plot of partial-least-squares (*PLS*) model B5 from Table 5

Table 5 Measured and predicted IEP for the eight PLS one-component models produced from the "best" replicate of the XPS overall spectra

Sample[a]	Measured IEP	Predicted IEP
B1	5.6	5.8
B2	6.8	6.6
B3	3.7	3.6
B4	7.6	7.0
B5	7.6	7.6
B6	4.1	3.8
B7	3.7	4.1
B8	3.7	3.5

[a] Independent validation sample

Discussion

The measurement of electrokinetic behaviour of colloidal particles is a sensitive method to study the surface chemistry of solid/liquid interfaces. Colloids in aqueous suspensions, such as oxides, develop electric charges on their surfaces as a result of charge-transfer processes responsible for maintaining electrochemical equilibrium between the solid surface and the solution. Small changes in the relative amount of chargeable surface groups of the colloidal particles are expected to change the electrokinetic potentials and/or the IEP. The difference in IEPs of these lanthanum chromite powders is therefore likely to be explained by the different type and content of atoms on the surface.

The processes that normally occur in aqueous solutions are surface hydration and dissociation of surface hydroxyl groups [21]. The negative charge on the oxide originates from acidic dissociation of the surface hydroxyl group. The positive charge arises from the addition of a proton to the neutral hydroxyl group

$$\text{AB-(OH)}_{3(\text{surface})} + 3\text{H}_2\text{O} \Leftrightarrow \text{AB-(O)}^{3-}_{3(\text{surface})} + 3\text{H}_3\text{O}^+ \quad (1)$$

$$\text{AB-(OH)}_{3(\text{surface})} + 3\text{H}_2\text{O} \Leftrightarrow \text{AB-(OH)}^{3+}_{3(\text{surface})} + 3\text{OH}^- \quad (2)$$

where AB-(OH)_3 designates a metal oxide such as lanthanum (A)-chromite(B). Equations (1) and (2) clearly show that changes in the concentration of acid or base affect the surface charge on the oxide and hence

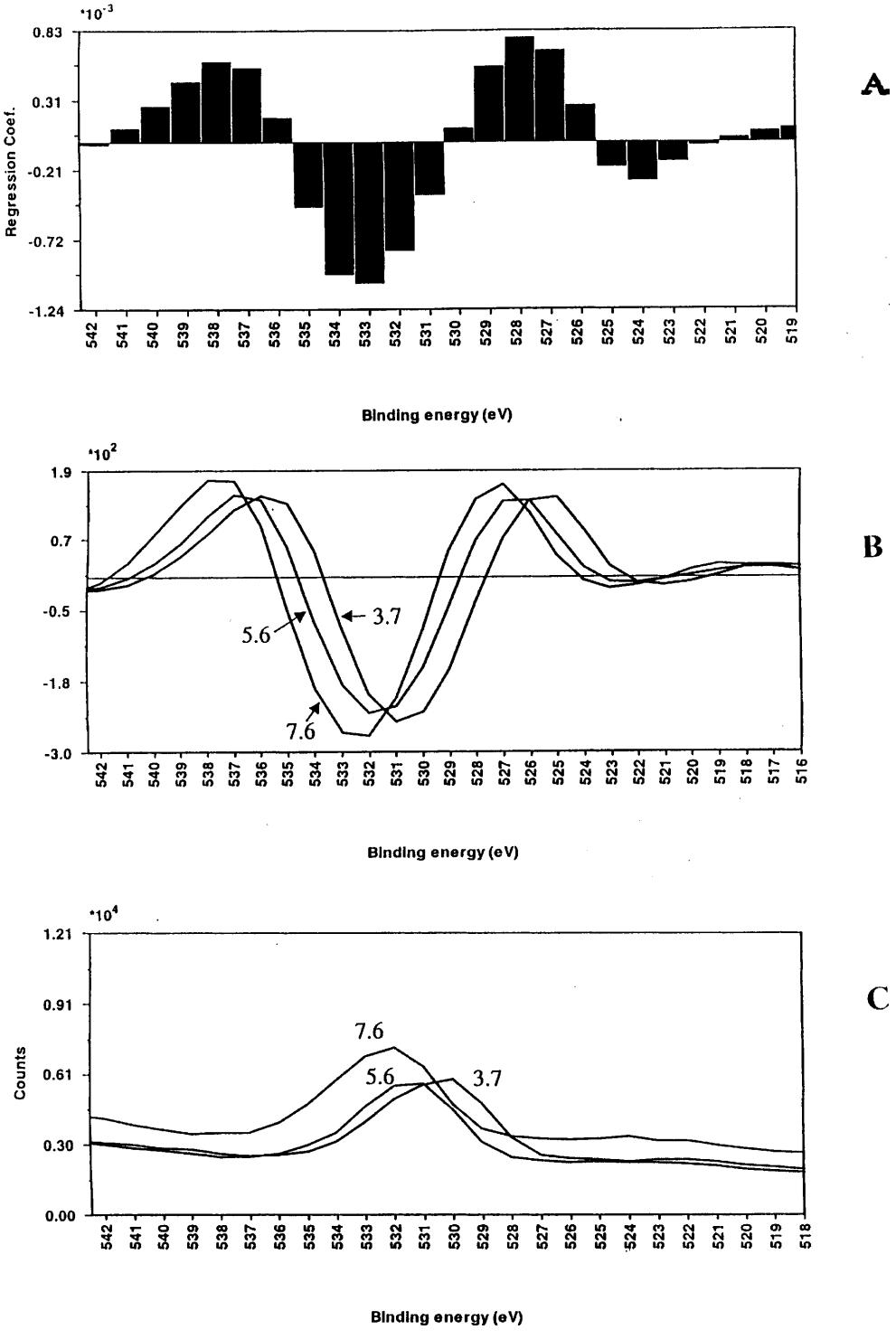

Fig. 12 **A** Regression coefficient plot of PLS model B5 from Table 5 for the oxygen peak, **B** second-order differentiated XPS spectra, oxygen peak area, for three powders with IEP values 3.7, 5.6 and 7.6, and **C** oxygen peak XPS spectra (untreated) for the same three powders

the electrokinetic potential. The determination of pH_{IEP}, as traditionally determined in water, may therefore serve as a general guide to the ability of the surface to lose or attract protons. Generally, more acidic oxides will have low, and basic oxides will have high, pH_{IEP} values. If the cations A or B have low positive surface charge density $AB(OH)_3$ is basic [22] forming $AB(OH)_3^{3+}$ and OH^- (see Eq. 2). If A or B have high positive surface charge density $AB(OH)_3$ is acidic, giving $AB(O)_3^{3-}$ and H_3O^+.

The results from PCA of the deconvoluted XPS data clearly showed that the IEP increases with increasing relative amount of La and O on the surface, and the

regression coefficient plot, Fig. 11, also showed that La and O contributed most in the PLS model.

When $LaCrO_3$ is doped with Ni or Zn on Cr and there is no doping on the most basic La site the highest IEP value, 7.6, is achieved. By doping on the La site with Ca the IEP decreases and it is seen that by increasing the amount of Ca dopant and thereby subsequently decreasing the amount of La the IEP decreases to 6.8 and 5.6, respectively. Ca will form highly basic oxide on the surface and we see that increasing the amount of Ca doping in the powder here seems to decrease surface basicity. One explanation for this is that La may form more basic oxides because of its larger radius and, hence, lower positive charge density than Ca. Another explanation is that even though the powder is Ca-doped it is still La that dominates on the powder surface.

Contradictory to the theory of surface charge density doping the basic Sr oxide shows IEP values form 3.7 to 4.1. A possible explanation for this is that Sr substitution for La in $LaCrO_3$ lowers the crystallographic transformation temperature of orthorhombic to rhombohedral [23] from 240 °C down to room temperature. This will affect the surface properties and consequently the IEP. Ni or Ca substitution raises the transformation temperature [24]. The Sr/Ni powder has an IEP value somewhat higher than all the other Sr-doped powders, which again can be understood from the crystallographic transformation. Mg substitution does not affect the orthorhombic-rhombohedral transformation temperature [25].

As far as we know there is little or no published data on lanthanum chromite electrokinetic behaviour in water for comparison.

What is apparent from these mobility measurements is that manipulation of the $LaCrO_3$ interconnect properties by the use of different types and amounts of dopants may significantly change the acidic or basic character of the powder surface, thereby giving altered conditions for conventionally used additives such as dispersant, plasticser and/or binder. A dispersant that seems to be an optimum choice for one type of doped powder may not be the best for a powder only differing in the type of dopant. To be able to choose the best type of dispersant for a powder, knowledge about the IEP may be of importance.

PCA of the XPS data revealed that differentiating the overall spectra, prior to extraction of the latent variables, gave the highest percentage explained variance and a clustering of the powders in agreement with PCA of the deconvoluted XPS data. This classification seems reasonable with regard to the powders' IEPs. The difference in percentage explained variance from the deconvoluted model to the differentiated XPS overall spectra shows that some information, with regard to the powders' surface composition, may be lost during the deconvolution procedure.

Multivariate regression of the IEP is significantly improved when using the overall spectra instead of the data from the deconvolution of XPS. The predictive errors of the models composed of the overall spectra are promising when considering that the measured IEPs have been determined with an accuracy of $pH_{IEP} \pm 0.3$. The accuracy of XPS for quantification is normally considered not to be better than 10% when relative surface composition values from deconvolution are obtained. By using the overall spectra directly the signal-to-noise ratio is higher compared to using the detail spectra, as is done in the traditional deconvolution procedure. No subjective criterion is used in latent variable decomposing in contrast to deconvolution analysis. Instead, the covariance structure between spectra and the response is used.

Conclusion

By using multivariate data analysis we have been able to model and predict the IEP values of the powders. Overall XPS spectra in combination with multivariable analysis gave better results than from the conventional deconvolution procedure. To use the overall XPS spectra directly is very rapid, nonsubjective and an efficient way of obtaining valuable information about the powder's acidic or basic surface in ceramic process control.

It was found that high La and O content at the surface corresponded to high IEPs.

Acknowledgements The authors thank Sissel Jørgensen for performing the XPS measurements, and for valuable discussions on the results. Gro Stakkestad would like to thank the Norwegian Research Council (NFR) for a doctor of science grant. The Zetasizer 4, Malvern Instruments, UK was also financed by the NFR.

References

1. Stakkestad G, Faaland S, Sigvartsen T (1996) Phase Transitions 58:159
2. Faaland S, Stakkestad G, Bardal A, Sigvartsen T, Høier R (1996) In: Poulsen FW, Bonanos N, Linderoth S, Mogensen M, Zachau-Christiansen B (eds) Proceedings of the 17th Risö International Symposium on Materials Science, Risö National Laboratory, p 241
3. Lange FF (1989) J Am Ceram Soc 72:3
4. Stakkestad G, Sjöblom J, Grung B, Sigvartsen T (1998) Colloid Polym Sci
5. Clark DT, Feast WJ (eds) (1978) Polymer surfaces. Wiley, New York, pp 309–351
6. Briggs D, Seah MP (eds) (1983) Practical surface analysis. Wiley, New York, pp 445–474

7. Lin AWC, Armstrong NR, Kuwana T (1977) Anal Chem 49:1228
8. Wagner CD, Rigg WM, Davis LE, Moulder JF, Muilenberg GE (1979) Handbook of X-ray photoelectron spectroscopy. Perkin-Elmer
9. Vandeginste BGM, DeGalan L (1975) Anal Chem 47:2124
10. Maddams WF (1980) Appl Spectrosc 34:245
11. Koenig MF, Grant JT (1986) J Electron Spectrosc Relat Phenom 41:145
12. Scierka JS, Proctor A, Houalla M, Fiedor JN, Hercules DM (1993) Surf Interface Anal 20:901
13. Oswald S, Baunack S (1997) Surf Interface Anal 25:942
14. hrlund Å, Hjertson L, Jacobsson SP (1997) Surf Interface Anal 25:105
15. Wold S, Esbensen K, Geladi P (1987) Chemom Intell Lab Syst 2:37
16. Wold S, Albano C, Dunn W, Edlund U, Esbensen K, Geladi P, Hellberg S, Johanson E, Lindberg W, Sjöström M (1984) In: Kowalski BR (ed) Chemometrics: mathematics and statistics in chemistry. Reidel, Dordrecht, p 17
17. Martens H, Næs T (1991) Multivariate calibration. Wiley, Chichester
18. Manne R (1987) Chemom Intell Lab Syst 2:187
19. Savitzky A, Golay MJE (1964) Anal Chem 36:1627–1639
20. Reartes GB, Morando PJ, Blesa MA, Hewlett PB, Matijevic E (1995) Langmuir 11:2277
21. Hunter RJ (1981) Zeta potential in colloid science: principles and applications. Academic Press, London
22. Douglas B, McDaniel D, Alexander J (1994) Concepts and models of inorganic chemistry. Wiley, New York
23. Khattak CP, Cox DE (1977) Matter Res Bull 12:463
24. Tolochko SP, Kononyuk IF, Lyutsko VA, Zonov Yu G (1987) Inorg Mater 23:1342
25. Srilomsak S, Schilling DP, Anderson HU (1989) In: Singal SC (ed) Proceedings of the 1st International Symposium on Solid Oxide Fuel Cells. The Electrochemical Society Pennington, New Jersey, p 129